Iran J Sci Technol Trans Electr Eng (2018) 42:95–105
https://doi.org/10.1007/s40998-018-0051-y

RESEARCH PAPER

Presenting an Object-Based Approach Using Image Edges to Detect Building Boundaries from High Spatial Resolution Images

Iman Khosravi[1] · Mehdi Momeni[1]

Received: 5 May 2016 / Accepted: 5 January 2018 / Published online: 19 January 2018

Abstract
Although various building detection algorithms from high spatial resolution satellite (HSRS) images have been presented in recent years, there are yet some difficulties to detect building boundaries for mapping purposes. The present study aims to propose a new approach to detect building boundaries from HSRS images by focusing on higher detection rates. The approach utilizes the idea of object-based image processing. However, it has an innovative vision using image edges instead of traditional image segments as objects. To evaluate the efficiency of the proposed approach, two datasets which have different contrast between building and non-building areas, are used: the first dataset has a high contrast between building and non-building areas (HC) and second has a low contrast (LC). The results are compared with the results of two segmentation-based algorithms, i.e., classification based on edge-based segmentation (CBES) and classification based on multi-resolution segmentation (CBMS). The comparisons indicate higher efficiency of the proposed approach for the HC dataset with 6–14% higher detection rate (lower omission error) than the two segmentation-based algorithms. For the LC dataset, the proposed approach is already more efficient than CBMS with 10–25% higher detection rate. However, it has lower efficiency than CBES with 15–36% higher omission errors. Though, the proposed approach is generally more robust than CBES and CBMS algorithms based on standard deviation values of evaluation metrics.

Keywords Object-based · Image edges · Segmentation · Building boundary · High spatial resolution

1 Introduction

At many municipal applications, the delineation of urban object boundaries, especially building boundaries, according to mapping standards is a vital task (Freire et al. 2014). Since 1999, the development of high spatial resolution satellite (HSRS) images has initiated an evolution in urban mapping, especially building detection. The more detailed content of HSRS images leads to the requirement of enhanced image processing methods. Heretofore, pixel-based image analysis (PBIA) has been used, which was not as efficient and reliable in the HSRS image processing (Wang et al. 2004; Aplin and Smith 2011; Khosravi et al. 2014). Gradually, object-based image analysis (OBIA), which employs groups of pixels, namely objects, as the processing units, has received considerable attention in the HSRS image processing. According to the most recent studies, OBIA methods have been more effective and reliable than the traditional PBIA methods for HSRS image processing (Cleve et al. 2008; Im et al. 2008; Blaschke 2010; Johansen et al. 2010; Lu et al. 2010; Pu et al. 2011; Meng et al. 2012; Hernando et al. 2012; Khosravi et al. 2014; Blaschke et al. 2014).

Until now, the only idea for creating image objects in the OBIA methods has been image segmentation (Khosravi et al. 2014). The process of image segmentation is to partition an image into non-intersecting regions such that each region is homogeneous and the union of any two adjacent regions is not homogeneous (Wang et al. 2010).

✉ Iman Khosravi
iman.khosravi@ut.ac.ir

Mehdi Momeni
momeni@eng.ui.ac.ir

[1] Department of Geomatics Engineering, Faculty of Civil Engineering and Transportation, University of Isfahan, Isfahan, Islamic Republic of Iran

Region-based segmentation algorithms are the most common types used in recent studies (e.g., Hu et al. 2005; Sebari and He 2009; Bouziani et al. 2010a, b; Wang et al. 2010; Meng et al. 2012; Sebari and He 2013). Some of the segmentation algorithms, e.g., multi-resolution segmentation, utilize pyramid image levels/scales (e.g., Baatz and Schape 2000; Benz et al. 2004; Chubey et al. 2006; Baatz et al. 2008; Lhomme et al. 2009; Taubenbock et al. 2010; Myint et al. 2011; Salehi et al. 2012; Nikfar et al. 2012; Dai et al. 2013; Khosravi et al. 2014; Han et al. 2014; Yin et al. 2015). Furthermore, some studies have recently used an edge-based segmentation algorithm (e.g., Kanjir et al. 2010; Hu and Weng 2011 and Khosravi et al. 2014).

Segmentation is a vantage for the OBIA methods as compared to PBIA; however, it may cause limitations in HSRS image processing due to over-segmentation and under-segmentation errors (Hay and Castilla 2008; Smith and Morton 2008; Liu and Xia 2010). Subsequently, these two errors can impact on classification based on resultant segments in two ways: first, all pixels in each mixed object have to be assigned to the same class. Second, over- or under-segmented objects change the geometrical properties of objects such as shape and area (Liu and Xia 2010). Therefore, segmentation errors may reduce reliability and increase commission and omission errors in delineation of object or building boundaries.

This study proposes utilization of edges as image objects, instead of segments, by focusing on higher detection rates for building boundaries. The objectives of the present study are: (1) to criticize the segmentation-based classification methods (the use of only segments as image objects) and (2) to use the edges as image objects for a special task, i.e., building boundary detection. In fact, the main aim of the paper is to find out whether the use of edges instead of segments as objects can improve the results of building boundary detection or not.

In the next section of the paper, we present the methodology of the paper. At first, we review two segmentation-based classification methods, namely classification based on edge-based segmentation (CBES) and classification based on multi-resolution segmentation (CBMS) to compare their results with the proposed method. Then, we introduce the proposed edge-object algorithm in theoretical detail. Section 3 presents the applied datasets. Then, using the datasets, implementation results of the three methods (CBMS, CBES and proposed) are compared together in Sect. 4. Section 5 contains the conclusions of the paper.

2 Methodology

2.1 Overview of Segmentation-Based Classification Methods

According to Holbling and Neubert (2008), the CBES algorithm has several steps. In the first step, CBES applies an edge-based segmentation to the image. Edge-based segmentation has two tuning parameters, namely a scale-level parameter (see Fig. 1a) and a merge-level parameter (see Fig. 1b). The trial and error based on visual inspection estimates the optimum values of the parameters. In our previous research, we examined several parameter combinations to make segment bounds close to building boundaries. At last, we chose 30 and 95 as optimum values for scale and merge levels, respectively, in our datasets (Khosravi et al. 2014). We use similar images in this paper; thus, the same values will be set here.

Based on image segmentation in the first step, CBES follows a supervised classification by training samples for urban classes such as "vegetation, shadow, bare land, roads and buildings". After selecting proper spectral and non-spectral attributes for segments, a support vector machine algorithm (Khodkar and Alavi 2016) with a Gaussian radial basis kernel is used to classify the produced objects according to our previous research (Khosravi et al. 2014). Figure 1c depicts the results of CBES in this step. Then, the building objects are extracted from the classified image (see Fig. 1d). Finally, any simple edge detector, such as Canny operator (Saryazdi 2016), can detect the boundary of buildings (see Fig. 1e).

Another segmentation-based algorithm, i.e., CBMS, has the similar steps with the CBES algorithm. However, it uses a different segmentation algorithm, namely multi-resolution segmentation. Multi-resolution segmentation has three tuning parameters: scale, shape and compactness (Baatz and Schape 2000). Again, trial and error procedure is used to estimate the optimum values. We set the values according to Khosravi et al. (2014). The segmented image is shown in Fig. 2a. Then we choose some proper object attributes such as "mean values for NDVI, green and brightness, area, length to width ratio, rectangular fit and shape index" (Khosravi et al. 2014). Then through a supervised task, the segments are classified using a fuzzy nearest neighbour classifier (see Fig. 2b). Finally, the building areas are separated from the classified image (see Fig. 2c) and the boundaries are detected using the Canny operator (see Fig. 2d).

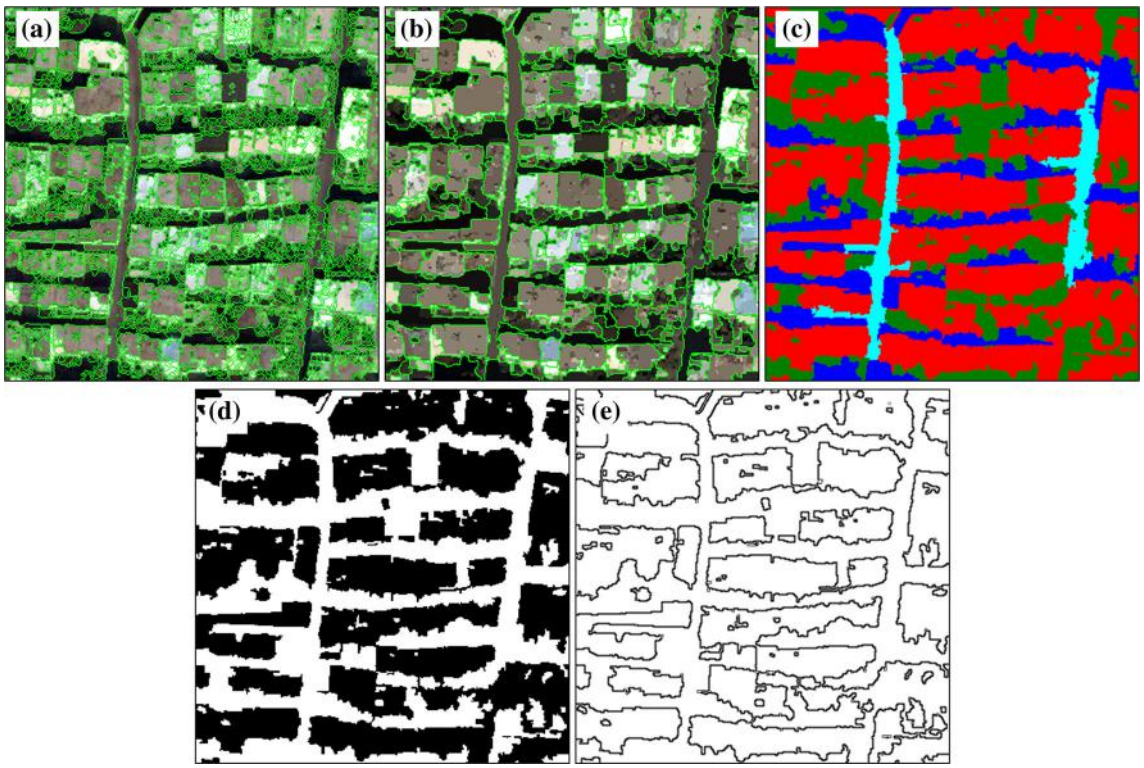

Fig. 1 The resultant images of CBES steps: **a** segmented image by edge-based segmentation at scale level, **b** segmented image by edge-based segmentation at merge level, **c** classified image by support vector machine method, **d** extracted building areas, **e** detected building boundaries by Canny operator

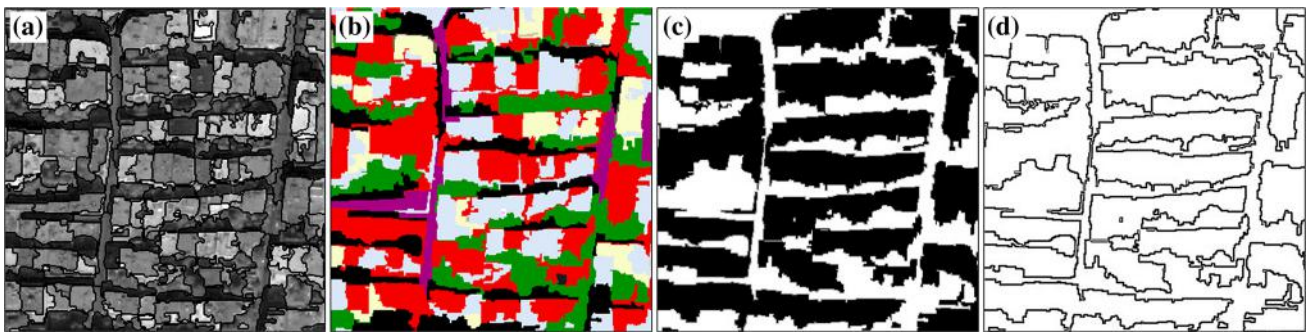

Fig. 2 The resultant images of CBMS steps: **a** segmented image by multi-resolution segmentation, **b** classified image by fuzzy nearest neighbor method, **c** extracted building areas, **d** detected Building boundaries by Canny operator

2.2 Proposed Method

Unlike previous OBIA studies, this paper proposes a rule object-based approach using edges (instead of segments) as objects. As depicted by Fig. 3, the outline of the proposed method contains four main steps: (1) eliminating non-building areas, (2) morphological post-processing, (3) defining edges as objects and (4) defining rules to classify edge objects.

2.2.1 Eliminating Non-building Areas

In an urban area, non-building areas often include vegetation, trees, green spaces, shadows and roads. After several experimental tests, we found that they have lower spectral reflectance than building roofs in the red band of the image. It can be seen in Fig. 4a. Therefore, an Otsu's thresholding algorithm is applied to the red image (Otsu 1979) to eliminate non-building areas. The resulting image

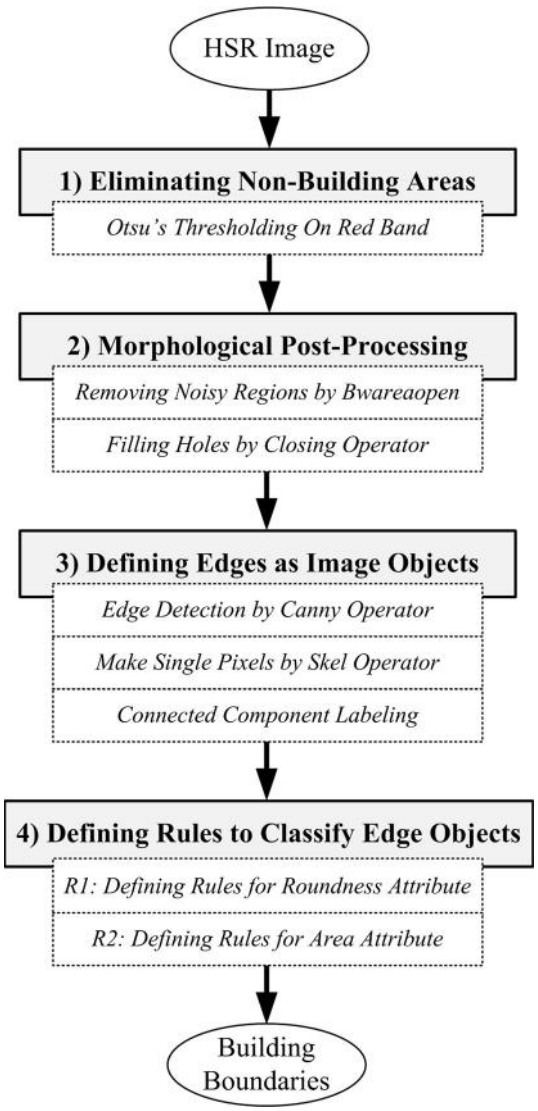

Fig. 3 The outline of the proposed method (Rule-based classification using edge objects)

is shown in Fig. 4b, in which the building areas layer is white and the non-building areas layer is black.

2.2.2 Morphological Post-Processing

Although most of the non-building areas are eliminated in the previous step, there are still some small non-building areas among the building layer. Some of them are marked by the ellipse in Fig. 4b. A bw-area-open morphological operator is applied to remove them. This operator is able to remove all objects whose their (i.e., the number of pixels) is lower than a predefined threshold (Gonzalez et al. 2004). Here, the value of the threshold is considered 100 pixels equivalent to 36 m^2 (for a pan-sharpened QuickBird image) because the smallest building area is around 40 m^2. Figure 5a shows the result of bw-area-open morphological processing. The second post-processing task is to fill small holes of the detected buildings that may be created due to chimneys, shadows and other small artifacts. It seems that a closing morphological operator (Gonzalez et al. 2004) will be helpful for solving this problem as the results are shown in Fig. 5a. For this operator, we use the square shape with a size of 2 by 2 pixels (in a pan-sharpened QuickBird image equal to 1.44 m^2) because the largest artifact area is around 1.5 m^2. Figure 5b shows the post-processed image of Fig. 4b using the two abovementioned morphological operators.

2.2.3 Defining Edges as Image Objects

Both this and the next steps are two main steps of the proposed algorithm. In this step, a Canny operator is applied to the binary image of Fig. 5b to extract the edges. Moreover, to make single-pixel edges, the skeletonization algorithm will be required. For this purpose, the Skel

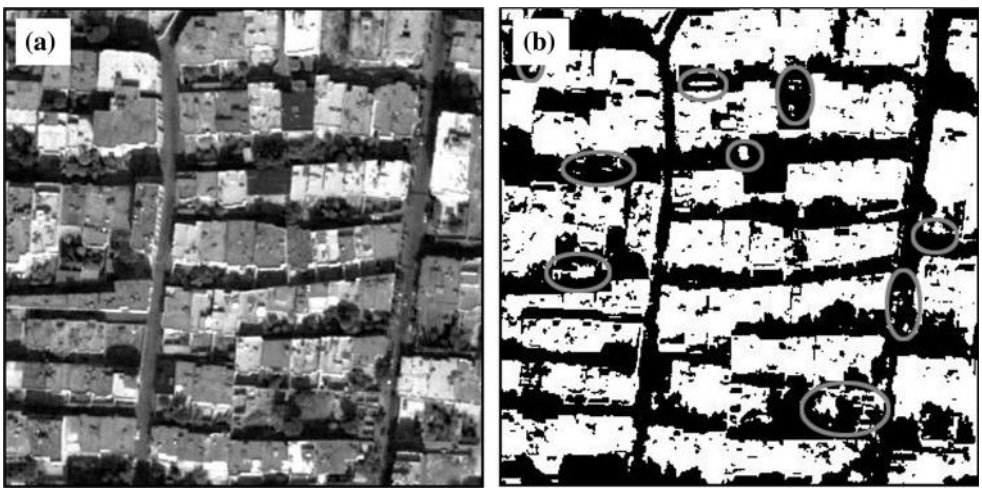

Fig. 4 **a** Red band image. Non-building areas have lower spectral reflectance than building areas. **b** Binary image by Otsu's thresholding. Non-building and building layers are black and white, respectively. Some small non-building areas still remain among buildings marked by ellipses

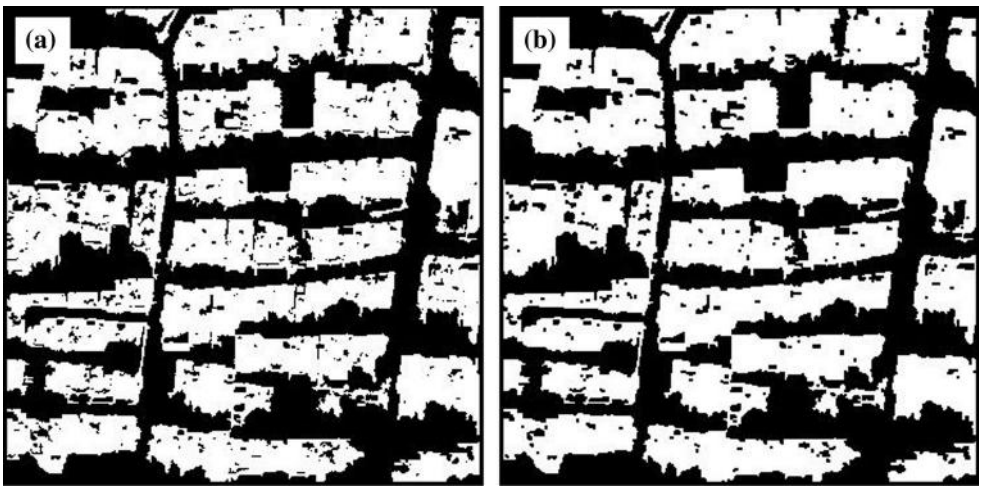

Fig. 5 **a** Removing small non-building areas by bw-area-open operator (threshold = 100 pixels), **b** filling holes of building areas by closing operator (2 × 2 pixels)

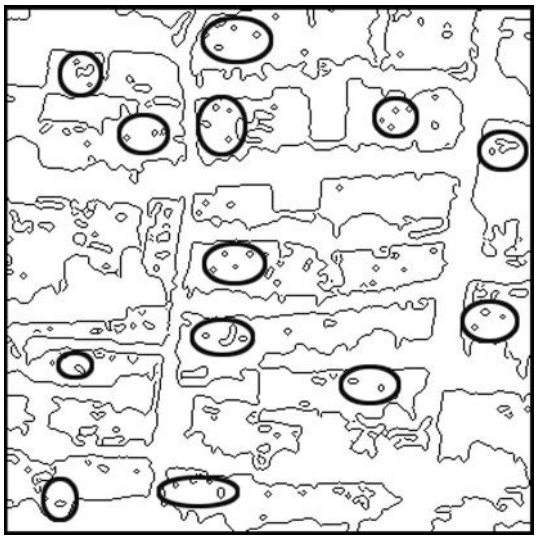

Fig. 6 Edges image produced by Canny operator and skeletonization algorithm. Ellipses show edges that are not building boundaries. They have generally small lengths

morphological operator is performed on the edges image (Gonzalez et al. 2004). The resultant image is shown in Fig. 6. Subsequently, the extracted edges can be defined as image objects. However, they are individual pixels and must be connected to form possible building boundaries. For this purpose, the concept of connected component labeling (Gonzalez et al. 2004) by 8 pixels connectivity is applied to Fig. 6. Hereto, this process creates primary edge objects.

2.2.4 Defining Rules to Classify Edge Objects

As can be seen in Fig. 6, some edges do not belong to building boundaries that are marked by the ellipses. Thus, these edges should be eliminated from the edges image. For this purpose, two rules are defined for two attributes of edge objects, i.e., roundness and area to classify them as follows:

Defining rule for roundness attribute (*R1*) The first attribute for edge objects is the roundness index (c) that can be defined as follows (Zhang and Zhu 2011):

$$c = \frac{P^2_{\text{Edge.object}}}{A_{\text{Edge.object}}}, \tag{1}$$

where P and A are the perimeter and area of the edge object, respectively. The roundness index is a geometric attribute that shows the degree to which the shape of an object is similar to a circle (Zhang and Zhu 2011). It is calculated for all edge objects of Fig. 6. Therefore, the first rule is defined as follows to remove the most rounded and small edges:

$$R1 : c > 40. \tag{2}$$

According to $R1$, the edge objects whose roundness attribute is smaller than 40, are removed from Fig. 6. The result is shown in Fig. 7a. The value of this threshold, which is computed by trial and error procedure, depends on spatial resolution of the image. In addition, it can be tuned based on the different urban areas and conditions.

Defining rule for area attribute (*R2*) After applying $R1$, some edges do not as yet belong to the building boundaries. They are marked by the ellipse in Fig. 7a. It is clear that their roundness attribute is more than 40, but they are still non-building boundary edges. The area attribute (i.e., the number of pixels) is efficient to remove them. Thus, the second rule is defined as follows:

$$R2 : A > 20. \tag{3}$$

Using $R2$, the edge objects that are smaller than 20 pixels (equals 7.2 m^2 on pan-sharpened QuickBird image), will be removed from image. The threshold of $R2$ depends on the spatial resolution of the image and it is tuned by considering the smallest area of the buildings. In this paper,

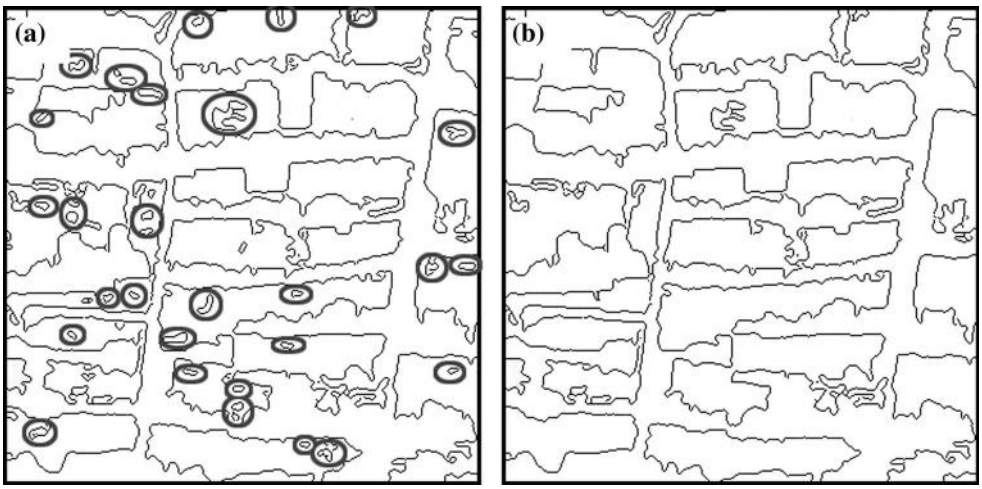

Fig. 7 **a** Image of rule 1: Removing edges which roundness attribute is smaller than 40. **b** Image of rule 2: Removing edges which area is smaller than 20 pixels (7.2 m^2)

it can be varied from 20 to 30 pixels (10.8 m^2) based on the different urban conditions. After all four abovementioned steps, the proposed object-based approach detects edges that belong to the building boundaries. The final results are shown in Fig. 7b.

3 Data and Study Area

To evaluate the proposed method, we use nine pan-sharpened Quickbird images of diverse urban and suburban regions of the city of Isfahan which were acquired on May 16, 2012 (Fig. 8a–j). Each image covers almost 45,000 m^2. The diversity of the images includes building alignment, density, shape, colour, intensity and heights. Furthermore, there are other urban objects around the building regions making the scene more complex such as roads, shadows, vegetation, green spaces and bare lands. In fact, the applied images are chosen based on the main challenges in an urban area referenced in the literature (Khosravi et al. 2014; Ghanea et al. 2014). To fairly compare the proposed methods with segmentation-based algorithms (CBES and CBMS), the images are categorized into two datasets based on the contrast between the building and non-building areas. Dataset 1 is the first six images (a–f) in which high contrast is seen between building and non-building areas and Dataset 2, i.e., the last three images (g–i) are the images of low contrast. These two datasets are abbreviated as HC and LC, respectively.

4 Experiments and Discussion

For evaluating the efficiency and reliability of the methods, the building boundaries detected by each are compared with their reference data, pixel by pixel. In this research, the reference building boundaries have been taken from a 1:2000 digital vector map which was prepared in 2012. To better assess the results, the digital vector map is rasterized so that the boundaries have one-pixel thickness around the vector lines. Then, common metrics such as the detection rate (DR), reliability (R) and false positive rate (FPR) or commission error are utilized to evaluate the methods (e.g., Shufelt 1999; Khoshelham et al. 2010; Xiao et al. 2012; Ozgun Ok 2013 Khosravi et al. 2014). Table 1 represents the definition of these metrics. The DR metric is related to the efficiency of the algorithms, so that a higher DR indicates the higher efficiency of an algorithm in the building boundaries detection. While the R and FPR metrics are related to the reliability of the algorithm, so that a high R and a low FPR imply the high reliability of the results (Khosravi et al. 2014).

Tables 2 and 3 present the assessment results of boundary detection of the three methods using both the HC and the LC datasets. In addition, their results are depicted in Fig. 9a–c. In the following, the details of the results are compared in terms of efficiency and reliability.

4.1 Discussion on Results of HC Dataset

Assessment of efficiency Referring to Table 2, the average DR of the proposed method is 67% that is 6 and 14% higher than each of CBES (61%) and CBMS (53%), respectively. In detail, the DR values of the proposed method are around 4–9% higher than the ones of CBES for 5 images (images b–f) and for image a, the difference between two methods is negligible (less than 2%). In addition, the DR values of the proposed method are much higher as compared to CBMS of all images (Fig. 9a). The difference is between 3% (for image f) and 48% (for image e).

The results imply that the proposed method is more efficient than two segmentation-based classification methods, especially compared to CBMS in the detection of building boundaries where there is high contrast between

Fig. 8 The dataset used in this study. **a–f** High contrast or HC group; **g–i** low contrast or LC group

Table 1 Metrics used for the assessment of the detection results (Khosravi et al. 2014)

Metrics	Formula	Explanations
Detection rate (DR)	$\mathrm{DR} = \frac{\mathrm{TP}}{\mathrm{TP}+\mathrm{FN}}$	TP refers to the pixels detected correctly as building boundaries
Reliability rate (R)	$R = \frac{\mathrm{TP}}{\mathrm{TP}+\mathrm{FP}}$	FP refers to the falsely detected building boundaries
False positive rate (FPR)	$\mathrm{FPR} = \frac{\mathrm{FP}}{\mathrm{TN}+\mathrm{FP}}$	FN refers to the pixels, which could not be detected as building boundaries although they exist in the reference data
		TN refers to the pixels detected correctly as non-building boundaries

building and non-building areas. This may be because of over/under-segmentation errors at CBES and CBMS that can lead to omission of some building boundaries.

Assessment of reliability From Table 2, the average R (reliability) metric of the proposed method is 9.5% that is around 1% higher than the R value for CBMS (8.8%) and only 0.1% lower than the *R* value for CBES (9.6%). Briefly, the *R* values of the proposed method are around 1–2% higher than the values of CBES in 4 images (images b, d, e and f) and also around 1–6% higher than the values

Table 2 The evaluation results of three object-based approaches at *HC* dataset

	DR values			*R* values			FPR values		
	Proposed Edge	CBES Segment	CBMS	Proposed Edge	CBES Segment	CBMS	Proposed Edge	CBES Segment	CBMS
a	66.80	68.75	61.26	7.75	10.17	7.68	24.08	18.69	22.67
b	63.50	58.27	57.62	10.63	9.09	10.47	20.92	22.95	19.41
c	72.60	63.37	61.95	8.48	10.27	9.77	26.38	18.64	19.27
d	64.57	60.90	57.57	10.27	9.86	10.00	26.66	26.62	24.76
e	68.28	59.47	20.47	10.35	9.17	4.08	26.11	27.97	22.84
f	63.51	56.89	60.45	9.70	9.29	10.84	29.07	27.38	24.52
AVG	66.54	61.28	53.22	9.53	9.64	8.81	25.54	23.71	22.25
STD	3.52	4.29	16.15	1.16	0.52	2.56	2.76	4.28	2.41

Table 3 The evaluation results of three object-based approaches at *LC* dataset

	DR values			*R* values			FPR values		
	Proposed Edge	CBES Segment	CBMS	Proposed Edge	CBES Segment	CBMS	Proposed Edge	CBES Segment	CBMS
g	49.31	64.08	60.71	6.68	8.59	10.03	31.17	35.82	28.58
h	52.69	67.83	28.24	6.88	7.87	4.38	23.97	26.69	20.65
i	54.12	89.67	43.63	4.52	15.53	7.16	29.52	13.22	15.32
AVG	52.04	73.86	44.19	6.03	10.66	7.19	28.22	25.24	21.52
STD	2.47	13.82	16.24	1.31	4.23	2.83	3.77	11.37	6.67

of CBMS in 4 images (images a, b, d and e). By contrast, the average FPR of the proposed method (26%) is 2 and 4% higher than the ones of CBES and CBMS, respectively. In addition, the FPR values of the proposed method are around 1–7% higher comparing to CBMS in all images. It can be clearly seen at the left part of the vertical line of Fig. 9c. However, our FPR values are around 2% lower compared to CBES at images b and e.

According to the results of *R* and FPR metrics, it can be concluded that the proposed method can be as reliable as and often more reliable than the segmentation-based methods where there is high contrast between building and non-building areas in the image. Therefore, the high efficiency and the relative high reliability of the proposed method at the HC dataset can be considered as one of the advantages of using simple edge objects instead of complex segment objects for detecting building boundaries.

4.2 Discussion on Results of LC dataset

Assessment of efficiency According to Table 3 for the LC dataset, the proposed method is still more efficient than CBMS in 2 of 3 images (images h and i), approximately 10–25% higher for the DR value. Furthermore, its average DR is 52% that is 8% higher than CBMS (44%). However, it has lower efficiency than CBES and 22% lower at the average DR. In addition, as can be seen in Fig. 9a, the DR value of the proposed method is around 15% (in images g and h) to 36% (in image i) lower than the CBES. Moreover, its value is around 11% lower than CBMS in image i (where there are complex blocks of buildings).

According to the results of LC dataset, the efficiency of the proposed algorithm is slightly lower than CBES in the detection of building boundaries. It can be said that the use of edges as objects may reduce the detection rate of building boundaries where there is low contrast between building and non-building areas in the image. However, the efficiency of the proposed method is much better than CBMS in some cases. It implies the relative efficiency of the proposed method in the detection of building boundaries.

Assessment of reliability From Table 3, the average R of the proposed method is 5 and 1% lower as compared to CBES and CBMS at LC dataset. In addition, the average FPR value of the proposed method is 3 and 7% higher than the values of CBES and CBMS, respectively. It is noteworthy that although there is low contrast between building and non-building areas in images g and h, the FPR values of the proposed method are nearly 4–5% lower than the CBES that is a positive and remarkable result for the proposed algorithm. One reason may be the segmentation errors that can cause commission errors at the building boundaries detected by CBES. However, at image i, the FPR value of the proposed method is 17 and 15% higher and its *R* value is 11 and 2% lower than CBES and CBMS, respectively.

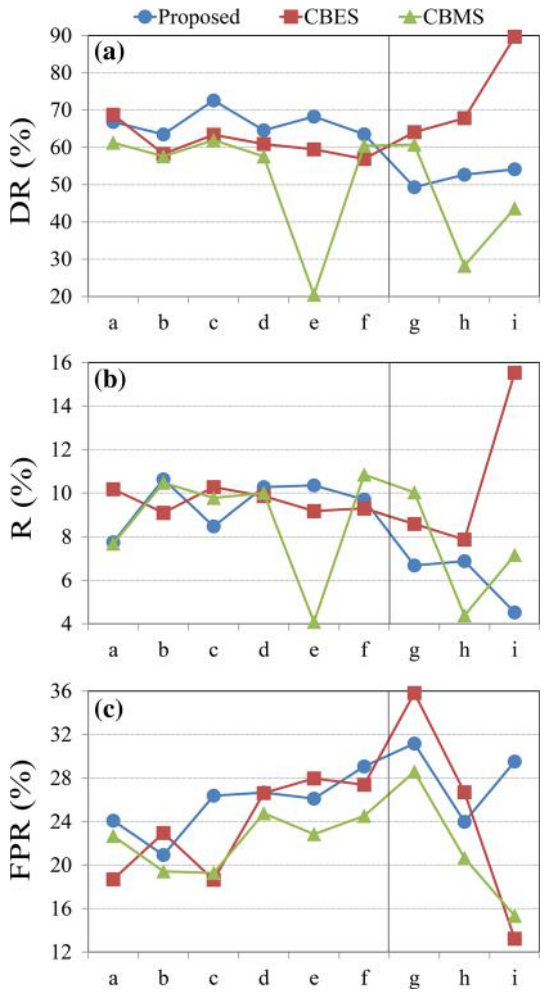

Fig. 9 The comparative evaluation among the proposed method (edge objects) and segmentation-based classifications (CBES and CBMS); The plots of **a** DR; **b** *R* and **c** FPR values

Therefore, based on the assessment of efficiency and reliability in the LC dataset, it can be fairly implied that the proposed method (the use of edges as image objects) may sometimes encounter difficulties in the detection of building boundaries where there is low contrast (or high spectral similarity) between building and non-building areas in the image. This issue can be due to the first step of the proposed method which is based on only spectral analysis (thresholding). It implies that the first step does not always hold.

4.3 General Discussion

Table 4 provides the evaluation results of three methods at all images. The average DR of the proposed algorithm is 62%, which is around 3% lower than CBES, however, it is 12% higher than the value for CBMS that is a remarkable advantage. In addition, the average R and FPR of the proposed method are almost equal with the values for the segmentation-based classification methods.

Concerning the proposed method, it can be found that the robustness of the proposed algorithm has been better than CBES and CBMS in all evaluation metrics due to lower standard deviation. This is clearly seen in Fig. 9 where the curves of the proposed method are often smoother than CBES and CBMS.

5 Conclusion

This paper studied the capability of defining edge (instead of segment) as image object at a special application, namely building boundaries detection. An object-based approach has been proposed for detecting building boundaries and it was compared with two segmentation-based classification methods (CBES and CBMS). In the images with high contrast between building and non-building areas, the use of the edges as image objects (proposed method) could produce 6–14% higher detection rates and fair reliability rates for building boundaries as compared to the use of the segments (CBES and CBMS). In other words, it can be claimed that the use of edge objects instead of segments can improve the results of building boundary detection where there is high contrast between building and non-building areas in the image. When there is low contrast between building and non-building areas in the images, the proposed method will be marginally more efficient than CBMS (with a 10–25% higher detection rate); however, it will be less efficient than CBES (with 15–36% higher omission errors). In this low contrast case, the reliability of the proposed method is slightly lower than the segmentation-based algorithms although it sometimes has higher relative efficiency than segmentation-based algorithms in the detection of building boundaries. In addition, the proposed algorithm is more

Table 4 The evaluation results of three object-based approaches at all images

	DR values			*R* values			FPR values		
	Proposed Edge	CBES Segment	CBMS	Proposed Edge	CBES Segment	CBMS	Proposed Edge	CBES Segment	CBMS
AVG	61.70	65.47	50.21	8.36	9.98	8.27	26.43	24.22	22.00
STD	7.62	9.94	15.78	2.08	2.21	2.60	3.18	6.66	3.86

robust than two segmentation-based classification algorithms in all evaluation metrics (due to lower standard deviation values) so that it can be considered as an advantage of the proposed object-based method.

We finally claim that the proposed method which used the simpler objects (edges) and less bothersome processing approach (morphology and thresholding) than the traditional object-based approach could produce more efficient and relatively reliable results. It is the answer to the question presented at the end of Introduction: "whether the use of edges instead of segments as objects can improve the results of building boundary detection or not". The simplicity and the ease of the proposed method can be considered as its main advantage.

References

Aplin P, Smith GM (2011) Introduction to object-based landscape analysis. Int J Geogr Inf Sci. 25:869–875

Baatz M, Schape A (2000) Multiresolution segmentation–an optimization approach for high quality multi-scale image segmentation. In: Strobl J et al (eds) Angewandte geographis informations verarbeitung XII. AGIT Symposium, Germany, pp 12–23

Baatz M, Hoffmann C, Willhauck G (2008) Progressing from object-based to object-oriented image analysis. In: Blaschke T, Lang S, Hay GJ (eds) Object-based image analysis. Springer, Berlin, pp 29–42

Benz UC, Hofmann P, Willhauck G, Lingenfelder I, Heynen M (2004) Multi-resolution, object-oriented fuzzy analysis of remote sensing data for GIS-ready information. ISPRS J Photogramm Remote Sens 58:239–258

Blaschke T (2010) Object based image analysis for remote sensing. ISPRS J Photogramm Remote Sens. 65:2–16

Blaschke T, Hay GJ, Kelly M, Lang S, Hofmann P, Addink E, Feitosa RQ, van der Meer F, van der Werff H, van Coillie F, Tiede D (2014) Geographic object-based image analysis—towards a new paradigm. ISPRS J Photogramm Remote Sens 87:180–191

Bouziani M, Goita K, He D-C (2010a) Automatic change detection of buildings in urban environment from very high spatial resolution images using existing geodatabase and prior knowledge. ISPRS J Photogramm Remote Sens 65:143–153

Bouziani M, Goita K, He D-C (2010b) Rule-based classification of a very high-resolution image in an urban environment using multispectral segmentation guided by cartographic data. IEEE Trans Geosci Remote Sens 48:3198–3211

Chubey MS, Franklin SE, Wulder MA (2006) Object-based analysis of Ikonos-2 imagery for extraction of forest inventory parameters. Photogramm Eng Remote Sens 72:383–394

Cleve C, Kelly M, Kearns FR, Moritz M (2008) Classification of the wildland–urban interface: a comparison of pixel- and object-based classifications using high-resolution aerial photography. Comput Environ Urban Syst 32:317–326

Dai Q, Zheng C, Sun D, Wang L (2013) MRF model with adaptive multiresolution for image segmentation. In: Proceeding. SPIE 8761, PIAGENG 2013: image-processing and photonics for agricultural engineering, p. 876107

Freire S, Santos T, Navarro A, Soares F, Silva JD, Afonso N, Fonseca A, Tenedório J (2014) Introducing mapping standards in the quality assessment of buildings extracted from very high-resolution satellite imagery. ISPRS J Photogramm Remote Sens 90:1–9

Ghanea M, Moallem P, Momeni M (2014) Automatic building extraction in dense urban areas through GeoEye multispectral imagery. Int J Remote Sens 35(13):5094–5119

Gonzalez RC, Woods RF, Eddins SL (2004) Digital image-processing using MATLAB, 2nd edn. Prentice-Hall, Inc, Upper Saddle River

Han N, Du H, Zhou G, Sun X, Ge H, Xu X (2014) Object-based classification using SPOT-5 imagery for Moso bamboo forest mapping. Int J Remote Sens 35(3):1126–1142

Hay GJ, Castilla G (2008) Geographic object-based image analysis (GEOBIA): a new name for a new discipline. In: Blaschke T, Lang S, Hay G (eds) Object-based image analysis. Lecture notes in geoinformation and cartography. Springer, Berlin, Heidelberg, pp 75–89. https://doi.org/10.1007/978-3-540-77058-9_4

Hernando A, Arroyo LA, Velazquez J, Tejera R (2012) Object-based image analysis for mapping natura 2000 habitats to improve forest management. Photogramm Eng Remote Sens 78:991–999

Holbling D, Neubert M (2008) ENVI feature extraction 4.5. Snapshot. Business 7:48–51

Hu X, Weng Q (2011) Impervious surface area extraction from IKONOS imagery using an object-based fuzzy method. Geocarto Int. 26:3–20

Hu X, Vincent Tao C, Prenzel B (2005) Automatic segmentation of high-resolution satellite imagery by integrating texture, intensity, and color features. Photogramm Eng Remote Sens 71:1399–1406

Im J, Jensen JR, Tullis JA (2008) Object–based change detection using correlation image analysis and image segmentation. Int J Remote Sens 29:399–423

Johansen K, Arroyo LA, Phinn S, Witte C (2010) Comparison of geo-object based and pixel-based change detection of riparian environments using high spatial resolution multi-spectral imagery. Photogramm Eng Remote Sens. 76:123–136

Kanjir U, Veljanovski T, Marsetic A, Ostir K (2010) Application of object based approach to heterogeneous land cover/use. Int Arch Photogramm Remote Sens Spat Inf Sci 38:4

Khodkar Z, Alavi SM (2016) Target classification enhancement in VHF radar using support vector machine. Iran J Sci Technol Trans Electr Eng 40(1):51–62

Khoshelham K, Nardinocchi C, Frontoni E, Mancini A, Zingaretti P (2010) Performance evaluation of automated approaches to building detection in multi-source aerial data. ISPRS J Photogramm Remote Sens 65:123–133

Khosravi I, Momeni M, Rahnemoonfar M (2014) Performance evaluation of object-based and pixel-based building detection algorithms from very high spatial resolution imagery. Photogramm Eng Remote Sens 80(5):519–523

Lhomme S, He D-C, Weber C, Morin D (2009) A new approach to building identification from very-high-spatial-resolution images. Int J Remote Sens 30:1341–1354

Liu D, Xia F (2010) Assessing object-based classification: advantages and limitations. Remote Sens Lett 1:187–194

Lu D, Hetrick S, Moran E (2010) Land cover classification in a complex urban-rural landscape with QuickBird imagery. Photogramm Eng Remote Sens. 76:1159–1168

Meng X, Currit N, Wang L, Yang X (2012) Detect residential buildings from Lidar and aerial photgraphs through object-oriented land-use classification. Photogramm Eng Remote Sens 78:35–44

Myint SW, Gober P, Brazel A, Grossman-Clarke S, Weng Q (2011) Per-pixel vs. object-based classification of urban land cover extraction using high spatial resolution imagery. Remote Sens. Env. 115:1145–1161

Nikfar M, Valadan-Zoej MJ, Mohammadzadeh A, Mokhtarzade M, Navabi A (2012) Optimization of multiresolution segmentation by using a genetic algorithm. J Appl Remote Sens 6:063592

Otsu N (1979) A threshold selection method from gray level histogram. IEEE Trans Syst Man Cybernet 9:62–66

Ozgun Ok A (2013) Automated detection of buildings from single VHR multispectral images using shadow information and graph cuts. ISPRS J Photogramm Remote Sens 86:21–40

Pu R, Landry S, Yu Q (2011) Object-based urban detailed land cover classification with high spatial resolution IKONOS imagery. Int J Remote Sens 32:3285–3308

Salehi B, Zhang Y, Zhong M, Dey V (2012) Object-based classification of urban areas using VHR imagery and height points ancillary data. Remote Sens. 4:2256–2276

Saryazdi S (2016) An optimal recursive step edge detector. Iran J Sci Technol Trans Electr Eng 40(1):35–44

Sebari I, He D-C (2009) Approach to nonparametric cooperative multiband segmentation with adaptive threshold. Appl Opt 48(20):3967–3978

Sebari I, He D-C (2013) Automatic fuzzy object-based analysis of VHSR images for urban objects extraction. ISPRS J Photogramm Remote Sens 79:171–184

Shufelt JA (1999) Performance evaluation and analysis of monocular building extraction from aerial imagery. IEEE Trans Pattern Anal Mach Intell 21(4):311–326

Smith G, Morton D (2008) Segmentation: the Achilles' heel of object–based image analysis? In: International archives of the photogrammetry, remote sensing and spatial information sciences, vol 38. No 4, p C1

Taubenbock H, Esch T, Wurm M, Roth A, Dech S (2010) Object-based feature extraction using high spatial resolution satellite data of urban area. J Spatial Sci 55:117–132

Wang L, Sousa WP, Gong P (2004) Integration of object-based and pixel-based classification for mapping mangroves with IKONOS imagery. Int J Remote Sens 25:5655–5668

Wang Z, Jensen JR, Im J (2010) An automatic region-based image segmentation algorithm for remote sensing applications. Environ Model Soft 25:1149–1165

Xiao J, Gerke M, Vosselman G (2012) Building extraction from oblique airborne imagery based on robust façade detection. ISPRS J Photogramm Remote Sens 68:56–68. https://doi.org/10.1016/j.isprsjprs.2011.12.006

Yin W, Yang J, Yamamoto H, Li C (2015) Object-based larch tree-crown delineation using high-resolution satellite imagery. Int J Remote Sens 36(3):822–844

Zhang R, Zhu D (2011) Study of land cover classification based on knowledge rules using high-resolution remote sensing images. Expert Syst Appl. 38:3647–3652